CSIAM Trans. Life Sci.
doi: 10.4208/csiam-ls.SO-2025-0007

Vol. **x**, No. x, pp. 1-26
xx 2025

Dynamics and Optimal Control of a Size-Structured Influenza Model Linking Within-Host and Between-Host

Ye Zheng[1,2], Junyuan Yang[1,2,*] and Xuezhi Li[3,*]

[1] *Complex Systems Research Center, Shanxi University, Taiyuan 030006, P.R. China.*
[2] *Shanxi Key Laboratory of Mathematical Techniques in Complex Systems, Shanxi University, Taiyuan 030006, P.R. China.*
[3] *School of Mathematics, Henan Normal University, Xinxiang 453007, P.R. China.*

Received 17 April 2025; Accepted 20 July 2025

Dedicated to Prof. Ma Zhien on the occasion of his 90th birthday, with deep gratitude for his contributions to research and for his encouragement to the younger generation.

Abstract. Multi-scale models improve the prediction of key epidemic factors and disease prevalence by capturing the interaction between individual immune responses and the spread of diseases among the population, helping to implement targeted control strategies for disease management. In this paper, we develop a novel size-structured influenza model based on the nested rules, aiming to explore how the replication of influenza virus affects its transmission at a population level. We calculate the basic reproduction numbers separately at the individual and population levels and rigorously prove the conditions under which the feasible equilibrium exists and is stable. Then, by evaluating the effectiveness of four measures consisting of individual antiviral treatment and population vaccination, we can determine an optimal treatment to minimize both the influenza cases and the total expenditure on influenza prevention. Numerical results reveal the complex interactions between the two interventions and the progression of the epidemic.

AMS subject classifications: 92D30, 92D25
Key words: Multi-scale influenza model, size-structure, optimal control, cost-effectiveness.

1 Introduction

Influenza is a kind of respiratory infectious disease. According to the different core protein types of the virus, it is classified into four types (A, B, C, and D). Among these, influenza A viruses (IAVs) transmit through droplets and aerosols, adhering to the ep-

*Corresponding author. *Email addresses:* yjyang@sxu.edu.cn (J.Yang), xzli66@126.com (X. Li)

ithelial cells of an individual's respiratory tract, proliferating and causing influenza. This can lead to pneumonia and potentially trigger other complications in patients [7]. During the 1918-1919 influenza pandemic, approximately a third of people were infected, which resulted in an estimated 100 million deaths worldwide [38]. To date, more than 15 million cases of respiratory tract infectious have been reported, resulting in approximately 200,000 hospitalizations attributed to IAVs [27]. Since the three globally well-known influenza pandemics in the 20th century, influenza has remained a major threat to global public health and economic development, despite the advances in medicine [20, 24, 35].

Within a host, the immune response is vital for limiting IAV propagation and mitigating the impact of influenza. Actually, IAV infection is usually self-limited due to the interaction between IAV replication and adaptive immunity [40]. The hemagglutinin (HA) of IAVs binds to receptors on the surface of a host cell, promoting endocytosis and the fusion of the virion with epithelial cells [34]. This process activates the host immune response and eliminates the infected epithelial cells. At the beginning of infection, the host immune system initiates an innate immune response. Natural killer cells (NK) and type I interferon (IFN)-I help resist viral invasion by promoting phagocytosis and clearance of IAV [2, 43]. Meanwhile, adaptive immune response is stimulated accordingly. $CD8^+$T cells (CTLs) initiate immune effects by recognizing and binding to viral antigens. Activated CTLs proliferate and differentiate into effector cells, which are capable of eliminating infected cells and clearing IAVs by releasing cytotoxic substances [37]. In the initial phase of infection with IAV in humans and animals, the viral load typically increases sharply within the first 1-2 days and subsequently reaches a peak. Although the severity of the illness may not be directly linked to the level of the virus loads or particular immune factors [14], a higher viral load can still impact how the disease evolves [5]. Comprehending the relationships among viral load, immune response, and progression of disease are significant for predicting health conditions of patients and implementing corresponding measures [30].

During an infectious process, when the virus invades the human body, there occurs an interaction between the evolution of the virus within a host and the dynamics of transmission among individuals. The immune-pathogen interactions within an individual are investigated by the within-host model, while disease transmission and strategies for its control are addressed by the between-host model. To build a bridge between the two scales, Gilchrist and Sasaki were the first to propose the multi-scale models, which have since been widely applied in the dynamic analysis of various chronic diseases [13], such as HIV [11], Cholera [29], Influenza [17, 28] and others [16, 21]. The main linking mechanism for within-host to between-host model is transmission rate, while the linking mechanisms for between-host to within-host model are pathogen loads and growth rates [8]. For parasitic infection models, the coupled models can help to determine critical conditions that lead to a rise in parasite within a host and provide strategic guidance for disease prevention and control [6]. Under such circumstances where predators are present or there is a competition among populations, the probable characteristics of diseases and their main roles in the dynamics of predator-prey were studied in [3]. The relationship

between pathogen invasion and the activation of individual immune response was investigated in [23, 25, 26], aiming to explore how individual's immunity influences epidemic outcomes. However, the studies mentioned above either assume a homogeneous environment or consider that age-since-infection increases synchronously over time. Actually, age-since-infection evolves within a host at hours, while the increase of time at a population level is day, week or year. Hence, they have a distinct inconsistence. Such phenomenon now is characterized by a size-structured model. Few studies have investigated the trade-offs of pathogens and the immune response in size-structured coupled systems.

In our research, we formulate an influenza immuno-epidemiological model by applying the nested law, which integrates the within-host and between-host dynamics. The former describes the interplay between IAV and immune response, while the latter is developed by a size-structured model, where the distribution of patients is structured by age-since-infection and time. In addition to the dynamical analysis of the model, we evaluate the contributions of antiviral treatment and vaccination on combating influenza by applying the optimal control theory. Recently, some researches on influenza modeling have focused on developing reasonable and effective control measures to minimize the spread of IAV infection [19, 22, 36, 39]. Two popular strategies for managing influenza spread are enhancing immunity through vaccination and reducing the risk of complications with antiviral therapy [15]. Serum antibodies play a major role in the protection provided by inactivated influenza vaccines [9], as vaccination boosts antibody levels and lowers the risk of disease from similar strains [32]. Antiviral treatment, involving neuraminidase inhibitors (NAIs) like oseltamivir and zanamivir, helps inhibit viral replication, reduce symptoms, shorten disease duration, and minimize complications [12]. In research on the optimal control of epidemics, the evaluation methods for various control strategies can be found in [18, 31, 33, 42].

The research conducted in this study is outlined below. In the next section, we propose a within-host model to describe IAV infection process at an individual level. In Section 3, we establish the connection mechanisms within a host and between hosts, propose a size-structured immuno-epidemiological model for influenza, and investigate the dynamical properties of the coupled systems. Section 4 introduces an optimal control system that incorporates antiviral therapy and vaccination strategies. We provide the derivation process of adjoint system and demonstrate the expression of its solution. We provide a numerical algorithm for the optimal control system and evaluate the effectiveness and cost of each strategy in Section 5. Lastly, a brief discussion is provided in Section 6.

2 Within-host model

To explore how pathogens interact with immune response within an individual, we simplify the within-host model proposed in [4] to develop our model. This model assumes

that the effect of cytotoxic $CD8^+$T cells on clearing infected cells is analogous to the process of virus elimination. Specifically, IAV infects epithelial cells in the respiratory tract, leading to viral replication, while CTLs recognize and kill virus, thereby limiting viral spread. By studying this interaction, we aim to gain a deeper understanding of the immune system's control over IAV infection and the factors that determine disease outcomes at an individual level. The dynamics of IAV and CTLs are represented by the following equations:

$$\begin{aligned}\frac{dP(x)}{dx}&=r_pP(x)\left(1-\frac{P(x)}{K_p}\right)-C_pP(x)E(x),\\ \frac{dE(x)}{dx}&=\frac{\beta_eE(x)P(x)}{P(x)+K_e}-C_eE(x)+S_e,\end{aligned}\tag{2.1}$$

where $P(\cdot)$ and $E(\cdot)$ represent the concentrations of IAV and pathogen-specific CTLs at age-of-infection x, respectively. The parameter K_p sets the upper limit for the self-replicating concentration of IAVs. r_p and $C_pE(\cdot)$ denote the rate of IAV replication and the rate at which IAV is eliminated by CTLs. S_e and C_e represent the rate of CTLs regeneration and decay, respectively. Additionally, the proliferation rate of CTLs is represented by β_e, and the half-saturation coefficient is K_e. The initial values for system (2.1) are

$$P(0)=P_0\geq 0,\quad E(0)=E_0\geq 0.$$

First, the positively invariant set of system (2.1) is

$$\Omega_1=\left\{(P_0,E_0)\in\mathbb{R}^2\,|\,0\leq P_0\leq K_p,0\leq E_0\leq\frac{S_e}{C_e-\beta_eK_p/(K_p+K_e)}\right\}.$$

Then, the immune reproduction number is defined as

$$\mathcal{R}_0^P=\frac{r_pC_e}{C_pS_e}.\tag{2.2}$$

According to [41, Lemma 2.1, Theorems 2.2 and 2.3], we conclude that when P^* satisfies the following equation:

$$\frac{1}{K_p}\left(1-\frac{\beta_e}{C_e}\right)P^2+\left[\frac{K_e}{K_p}+\frac{1}{\mathcal{R}_0^P}-\left(1-\frac{\beta_e}{C_e}\right)\right]P+\left(\frac{1}{\mathcal{R}_0^P}-1\right)K_e=0,\tag{2.3}$$

and if $\mathcal{R}_0^P>1$, then for all $\phi\in\Omega_1\backslash(0,S_e/C_e)$, the virus transmission equilibrium $E_*^P=(P^*,E^*)$ with $P^*\in(0,K_p)$ is globally asymptotically stable, where $E^*=(r_p/C_p)(1-P^*/K_p)$.

3 Between-host model

To analyze the transmission of influenza A in a population, we next develop a model that describes the interaction among individuals. The model extends the physiologically

structured model from [25]. We introduce two preventative strategies to reduce IAV infection: vaccination and antiviral medication. The transmission and recovery rates are used to link the dynamics between individuals and the population, enabling us to understand how these two scales work together to affect the IAV transmission.

The model consists of four groups: susceptible (S), vaccinated (V), infected (I) and recovered (R) individuals. The individuals who are infected have a density of $i(x,t)$ with age-since-infection x at time t. The probability of susceptible individuals acquiring an infection through contact with infected individuals is $S(t)\int_0^\infty \beta(x)i(x,t)dx$, while the probability of vaccination is φ. The immunity of vaccinated individuals will weaken over time and they will be reinfected at rate $\sigma V(t)\int_0^\infty \beta(x)i(x,t)dx$. Based on aforementioned mechanisms, we can propose the model as below

$$\frac{dS(t)}{dt} = \Lambda - \varphi S(t) - S(t)\int_0^\infty \beta(x)i(x,t)dx - \mu S(t), \tag{3.1a}$$

$$\frac{dV(t)}{dt} = \varphi S(t) - \sigma V(t)\int_0^\infty \beta(x)i(x,t)dx - \mu V(t), \tag{3.1b}$$

$$i_t(x,t) + \big(g(x)i(x,t)\big)_x = -\big(\gamma(x)+\mu\big)i(x,t), \tag{3.1c}$$

$$g(0)i(0,t) = S(t)\int_0^\infty \beta(x)i(x,t)dx + \sigma V(t)\int_0^\infty \beta(x)i(x,t)dx, \tag{3.1d}$$

$$\frac{dR(t)}{dt} = \int_0^\infty \gamma(x)i(x,t)dx - \mu R(t), \tag{3.1e}$$

where the recruitment rate is denoted by Λ, and μ represents the rate of natural death. The virus conversion rate is denoted by the function $g(\cdot)\in C^1(\mathbb{R}_+)$ with $g'(x)+\gamma(x)+\mu>0$ a.e $x\in\mathbb{R}_+$, while σ quantifies the influenza vaccine's inefficacy. The transmission function $\beta(\cdot)$ and treatment function $\gamma(\cdot)$ are functions of IAV loads and the sizes of immune cells, i.e.

$$\beta(\cdot) = \beta P(\cdot), \quad \gamma(\cdot) = \gamma E(\cdot),$$

where β and γ are scaler coefficients. The initial values of system (3.1) are

$$S(0) = S_0 \in \mathbb{R}, \quad I(x,0) = I_0(x) \in \mathbb{L}^1(\mathbb{R}_+), \quad V(0) = V_0 \in \mathbb{R}, \quad R(0) = R_0 \in \mathbb{R}.$$

Since the Eq. (3.1e) can be derived from the other equations, we directly analyze the simplified system below

$$\begin{aligned}
&\frac{dS(t)}{dt} = \Lambda - \varphi S(t) - S(t)\int_0^\infty \beta(x)i(x,t)dx - \mu S(t),\\
&\frac{dV(t)}{dt} = \varphi S(t) - \sigma V(t)\int_0^\infty \beta(x)i(x,t)dx - \mu V(t),\\
&i_t(x,t) + \big(g(x)i(x,t)\big)_x = -\big(\gamma(x)+\mu\big)i(x,t),\\
&g(0)i(0,t) = S(t)\int_0^\infty \beta(x)i(x,t)dx + \sigma V(t)\int_0^\infty \beta(x)i(x,t)dx.
\end{aligned} \tag{3.2}$$

Apparently, $E^0=(S^0,V^0,0)$ is the infection-free equilibrium of system (3.2), where

$$S^0=\frac{\Lambda}{\varphi+\mu},\quad V^0=\frac{\Lambda\varphi}{\mu(\varphi+\mu)}.$$

We linearize above system at E^0 to obtain the solution for $i(x,t)$.

$$i_t(x,t)+\big(g(x)i(x,t)\big)_x=-\big(\gamma(x)+\mu\big)i(x,t), \tag{3.3a}$$

$$g(0)i(0,t)=S^0\int_0^\infty\beta(x)i(x,t)dx+\sigma V^0\int_0^\infty\beta(x)i(x,t)dx. \tag{3.3b}$$

We make the assumption that $g'(x)<0$ and let $x=G(t)+C$ represent the characteristic curve of Eq. (3.3). Then, we have

$$G^{-1}(x-C)=\int_0^x\frac{ds}{g(s)},$$

and it satisfies that $G^{-1}(0)=0$ and $G^{-1}(\infty)=\infty$. We solve Eq. (3.3) as below

$$i(x,t)=\begin{cases} i\big(0,t-G^{-1}(x)\big)\Pi\big(G^{-1}(x)\big), & t>G^{-1}(x),\\ i_0\big(G(G^{-1}(x)-t)\big)\dfrac{\Pi\big(G^{-1}(x)\big)}{\Pi\big(G^{-1}(x)-t\big)}, & t<G^{-1}(x),\end{cases} \tag{3.4}$$

where

$$\Pi\big(G^{-1}(x)\big)=e^{-\int_0^{G^{-1}(x)}(\gamma(G(\xi))+g_x(G(\xi))+\mu)d\xi}.$$

Substituting $i(x,t)$ into the Eq. (3.3b), we have

$$\begin{aligned} i(0,t)&=\frac{S^0+\sigma V^0}{g(0)}\bigg(\int_0^{G(t)}\beta(x)i\big(0,t-G^{-1}(x)\big)\Pi\big(G^{-1}(x)\big)dx \\ &\qquad+\int_{G(t)}^\infty\beta(x)i_0\big(G(G^{-1}(x)-t)\big)\frac{\Pi\big(G^{-1}(x)\big)}{\Pi\big(G^{-1}(x)-t\big)}dx\bigg) \\ &=\frac{S^0+\sigma V^0}{g(0)}\int_0^t\beta\big(G(t-\omega)\big)\Pi(t-\omega)g\big(G(t-\omega)\big)i(0,\omega)d\omega \\ &\quad+\frac{S^0+\sigma V^0}{g(0)}\int_{G(t)}^\infty\beta(x)i_0\big(G(G^{-1}(x)-t)\big)\frac{\Pi\big(G^{-1}(x)\big)}{\Pi\big(G^{-1}(x)-t\big)}dx \\ &=\int_0^t K(t-\omega)i(0,\omega)d\omega+\frac{S^0+\sigma V^0}{g(0)}\int_{G(t)}^\infty\beta(x)i_0\big(G(G^{-1}(x)-t)\big)\frac{\Pi\big(G^{-1}(x)\big)}{\Pi\big(G^{-1}(x)-t\big)}dx, \end{aligned} \tag{3.5}$$

where

$$K(\omega)=\frac{S^0+\sigma V^0}{g(0)}\beta\big(G(\omega)\big)\Pi(\omega)g\big(G(\omega)\big).$$

By the knowledge of renewal equation in [10], we define the basic reproduction number of system (3.2) by

$$\begin{aligned}\mathcal{R}_0 &= \int_0^\infty K(\omega)d\omega = \frac{S^0+\sigma V^0}{g(0)}\int_0^\infty \beta\big(G(\omega)\big)\Pi(\omega)g\big(G(\omega)\big)d\omega \\ &= \frac{S^0+\sigma V^0}{g(0)}\int_0^\infty \beta\big(G(\omega)\big)e^{-\int_0^{G(\omega)}\frac{\gamma(s)+\mu+g_x(s)}{g(s)}ds}g\big(G(\omega)\big)d\omega \\ &= (S^0+\sigma V^0)\int_0^\infty \frac{\beta(x)}{g(x)}e^{-\int_0^x\frac{\gamma(s)+\mu}{g(s)}ds}dx, \end{aligned} \tag{3.6}$$

where $1/g(x)$ denotes the amount of time required for unit size growth. The exponential term $e^{-\int_0^x(\gamma(s)+\mu)/g(s)ds}$ represents the probability that an infected individual survives from size 0 to x. Hence, $\beta(x)e^{-\int_0^x(\gamma(s)+\mu)/g(s)ds}/g(x)$ describes the expected number of secondary infections caused by an individual at size x. Therefore, $\mathcal{R}_0$ quantifies the total number of secondary infections generated by a single infected individual throughout the course of infection within the population of susceptible $S^0+\sigma V^0$.

3.1 The existence of equilibria

Theorem 3.1. *$\mathcal{R}_0$ is defined in* (3.6)*. We have the following statements:*

(1) If $\mathcal{R}_0<1$, there is a disease-free equilibrium

$$E^0=(S^0,V^0,0)=\left(\frac{\Lambda}{\varphi+\mu},\frac{\Lambda\varphi}{\mu(\varphi+\mu)},0\right)$$

in system (3.2)*.*

(2) If $\mathcal{R}_0>1$, there are two equilibrium in system (3.2)*, i.e. the disease-free equilibrium E_0 and the epidemic equilibrium $E^*=(S^*,V^*,i^*(\cdot))$. The expressions for S^*,V^*,i^* are provided as proof.*

Proof. The epidemic equilibrium $E^*=(S^*,V^*,i^*(\cdot))$ satisfies

$$\Lambda-\varphi S^*-S^*\int_0^\infty\beta(x)i^*(x)dx-\mu S^*=0, \tag{3.7a}$$

$$\varphi S^*-\sigma V^*\int_0^\infty\beta(x)i^*(x)dx-\mu V^*=0, \tag{3.7b}$$

$$g(x)i_x^*(x)=-\big(\gamma(x)+g_x(x)+\mu\big)i^*(x), \tag{3.7c}$$

$$g(0)i^*(0)=S^*\int_0^\infty\beta(x)i^*(x)dx+\sigma V^*\int_0^\infty\beta(x)i^*(x)dx. \tag{3.7d}$$

Solving (3.7), we obtain

$$S^*=\frac{\Lambda}{\varphi+\mu+i^*(0)\displaystyle\int_0^\infty\beta(x)\Pi\big(G^{-1}(x)\big)dx}, \tag{3.8}$$

$$i^*(x)=i^*(0)e^{-\int_0^x \frac{\gamma(s)+g_X(s)+\mu}{g(s)}ds}=i^*(0)\Pi\big(G^{-1}(x)\big), \tag{3.9}$$

$$V^*=\frac{\varphi S^*}{\mu+\sigma i^*(0)\displaystyle\int_0^\infty \beta(x)\Pi\big(G^{-1}(x)\big)dx}. \tag{3.10}$$

Substituting (3.9) and (3.10) into the Eq. (3.7d), yields

$$\begin{aligned} g(0)i^*(0)&=(S^*+\sigma V^*)i^*(0)\int_0^\infty \beta(x)\Pi\big(G^{-1}(x)\big)dx \\ &=i^*(0)S^*\left(1+\frac{\sigma\varphi}{\mu+\sigma i^*(0)\displaystyle\int_0^\infty \beta(x)\Pi\big(G^{-1}(x)\big)dx}\right)\int_0^\infty \beta(x)\Pi\big(G^{-1}(x)\big)dx. \end{aligned} \tag{3.11}$$

If $i^*(0)\neq 0$, dividing both sides by $i^*(0)$, we have following expression of function Q:

$$1=\frac{S^*}{g(0)}\left(1+\frac{\sigma\varphi}{\mu+\sigma i^*(0)\displaystyle\int_0^\infty \beta(x)\Pi\big(G^{-1}(x)\big)dx}\right)\int_0^\infty \beta(x)\Pi\big(G^{-1}(x)\big)dx=:Q[i^*(0)]. \tag{3.12}$$

Apparently, $Q[i^*(0)]$ monotonically decreases as $i^*(0)$ increases and satisfies

$$\begin{aligned} \lim_{i^*(0)\to\bar{i}^*(0)} Q[i^*(0)]&=\frac{\Lambda\displaystyle\int_0^\infty \beta(x)\Pi\big(G^{-1}(x)\big)dx}{g(0)\left(\varphi+\mu+\bar{i}^*(0)\displaystyle\int_0^\infty \beta(x)\Pi\big(G^{-1}(x)\big)dx\right)} \\ &\quad\times\left(1+\frac{\sigma\varphi}{\mu+\sigma\bar{i}^*(0)\displaystyle\int_0^\infty \beta(x)\Pi\big(G^{-1}(x)\big)dx}\right) \\ &\leq\frac{\Lambda\displaystyle\int_0^\infty \beta(x)\Pi\big(G^{-1}(x)\big)dx}{g(0)\left(\varphi+\bar{i}^*(0)\displaystyle\int_0^\infty \beta(x)\Pi\big(G^{-1}(x)\big)dx\right)}\frac{\varphi+\bar{i}^*(0)\displaystyle\int_0^\infty \beta(x)\Pi\big(G^{-1}(x)\big)dx}{\bar{i}^*(0)\displaystyle\int_0^\infty \beta(x)\Pi\big(G^{-1}(x)\big)dx} \\ &=\frac{\Lambda}{g(0)}\frac{1}{\bar{i}^*(0)}=\frac{\mu}{(S^0+\sigma V^0)\bar{\beta}}<\frac{1}{\mathcal{R}_0}<1, \end{aligned}$$

where

$$\begin{aligned} &\bar{i}^*(0)=\frac{(S^0+\sigma V^0)\bar{\beta}\Lambda}{g(0)\mu},\quad \beta(\cdot)\leq\bar{\beta}, \\ &Q(0)=\int_0^\infty \frac{S^0+\sigma V^0}{g(0)}\beta\big(G(\omega)\big)\Pi(\omega)g\big(G(\omega)\big)d\omega=\mathcal{R}_0. \end{aligned}$$

Therefore, if $\mathcal{R}_0 > 1$, there is a unique positive solution to the equilibrium equation (3.12), which implies the existence of an endemic equilibrium $E^* = (S^*, V^*, i^*(\cdot))$. Otherwise, if the Eq. (3.12) has no positive solution, indicating that system (3.2) does not have an endemic equilibrium. □

3.2 Local stability of the disease-free equilibrium

Theorem 3.2. *The disease-free equilibrium E^0 is locally asymptotically stable when $\mathcal{R}_0 < 1$, and E^0 becomes unstable when $\mathcal{R}_0 > 1$.*

Proof. To investigate the stability of E^0, we introduce the following perturbations:

$$\bar{S}(t) = S(t) - S^0, \quad \bar{V}(t) = V(t) - V^0, \quad \bar{i}(x,t) = i(x,t).$$

Then we linearize system (3.2) and assume

$$\bar{S}(t) = \bar{S}e^{\lambda t}, \quad \bar{V}(t) = \bar{V}e^{\lambda t}, \quad \bar{i}(x,t) = \bar{i}(x)e^{\lambda t},$$

which yields

$$\lambda \bar{S} = -\varphi \bar{S} - S^0 \int_0^\infty \beta(x)\bar{i}(x)dx - \mu \bar{S}, \tag{3.13a}$$

$$\lambda \bar{V} = \varphi \bar{S} - \sigma V^0 \int_0^\infty \beta(x)\bar{i}(x)dx - \mu \bar{V}, \tag{3.13b}$$

$$\lambda \bar{i}(x) + g(x)\bar{i}_x(x) = -\big(\gamma(x) + g_x(x) + \mu\big)\bar{i}(x), \tag{3.13c}$$

$$g(0)\bar{i}(0) = (S^0 + \sigma V^0) \int_0^\infty \beta(x)\bar{i}(x)dx. \tag{3.13d}$$

The solution of $\bar{i}(x)$ can be expressed by

$$\bar{i}(x) = \bar{i}(0)e^{-\int_0^x \frac{\gamma(s)+g_x(s)+\mu+\lambda}{g(s)}ds}.$$

We substitute it to the Eq. (3.13d) and obtain

$$\begin{aligned} g(0)\bar{i}(0) &= (S^0 + \sigma V^0)\bar{i}(0) \int_0^\infty \beta(x) e^{-\int_0^x \frac{\gamma(s)+g_x(s)+\mu+\lambda}{g(s)}ds} dx \\ &= (S^0 + \sigma V^0)\bar{i}(0) \int_0^\infty \beta(x)\Pi\big(G^{-1}(x)\big) e^{-\lambda G^{-1}(x)} dx. \end{aligned} \tag{3.14}$$

Case 1: If $\bar{i}(0) \neq 0$, the following equation is derived

$$1 = \frac{S^0 + \sigma V^0}{g(0)} \int_0^\infty \beta(x)\Pi\big(G^{-1}(x)\big) e^{-\lambda G^{-1}(x)} dx =: H(\lambda). \tag{3.15}$$

(1) If $\lambda\in\mathbb{R}$, then $H(\lambda)$ monotonically decreases as λ increases and

$$\lim_{\lambda\to-\infty}H(\lambda)=+\infty.$$

Moreover, if $\mathcal{R}_0<1$, then

$$H(0)=\frac{S^0+\sigma V^0}{g(0)}\int_0^\infty\beta(x)\Pi\big(G^{-1}(x)\big)dx=\mathcal{R}_0<1.$$

Thus, $H(\lambda)=1$ has no non-negative real roots.

(2) If $\lambda\in\mathbb{C}$, assume $\Re\lambda\geq 0$, then

$$1=|H(\lambda)|\leq|H(\Re\lambda)|\leq|H(0)|=\mathcal{R}_0,$$

which contradicts with $\mathcal{R}_0<1$, so the real part of λ is negative.

Case 2: If $\tilde{i}(0)=0$, we obtain $\lambda=-\varphi-\mu$, which is derived from the Eq. (3.13a).

In a word, if $\mathcal{R}_0<1$, then any solution of Eq. (3.15) is either negative or has a negative real part, indicating that E^0 is locally asymptotically stable. Conversely, if $\mathcal{R}_0>1$, based on the properties of $H(\lambda)$, there is at least one positive solution to Eq. (3.15), implying that E^0 is unstable. □

3.3 Local stability of endemic equilibrium

Assuming $\mathcal{R}_0>1$ and linearizing system (3.2) at E^* with

$$\widetilde{S}(t)=S(t)-S^*,\quad \widetilde{V}(t)=V(t)-V^*,\quad \widetilde{i}(x,t)=i(x,t)-i^*(x),$$

we have

$$\begin{aligned}
&\frac{d\widetilde{S}(t)}{dt}=-\varphi\widetilde{S}(t)-\widetilde{S}(t)\int_0^\infty\beta(x)i^*(x)dx-S^*\int_0^\infty\beta(x)\widetilde{i}(x,t)dx-\mu\widetilde{S}(t),\\
&\frac{d\widetilde{V}(t)}{dt}=\varphi\widetilde{S}(t)-\sigma\widetilde{V}(t)\int_0^\infty\beta(x)i^*(x)dx-\sigma V^*\int_0^\infty\beta(x)\widetilde{i}(x,t)dx-\mu\widetilde{V}(t),\\
&\widetilde{i}_t(x,t)+\big(g(x)\widetilde{i}(x,t)\big)_x=-\big(\gamma(x)+\mu\big)\widetilde{i}(x,t),\\
&g(0)\widetilde{i}(0,t)=\big(\widetilde{S}(t)+\sigma\widetilde{V}(t)\big)\int_0^\infty\beta(x)i^*(x)dx+(S^*+\sigma V^*)\int_0^\infty\beta(x)\widetilde{i}(x,t)dx.
\end{aligned}\tag{3.16}$$

We seek solutions of the form $\widetilde{S}(t)=\widetilde{S}e^{\lambda t}$, $\widetilde{V}(t)=\widetilde{V}e^{\lambda t}$ and $\widetilde{i}(x,t)=\widetilde{i}(x)e^{\lambda t}$. Substituting the appropriate form in (3.16) yields

$$\lambda\widetilde{S}=-\varphi\widetilde{S}-\widetilde{S}\int_0^\infty\beta(x)i^*(x)dx-S^*\int_0^\infty\beta(x)\widetilde{i}(x)dx-\mu\widetilde{S},\tag{3.17a}$$

$$\lambda\widetilde{V}=\varphi\widetilde{S}-\sigma\widetilde{V}\int_0^\infty\beta(x)i^*(x)dx-\sigma V^*\int_0^\infty\beta(x)\widetilde{i}(x)dx-\mu\widetilde{V},\tag{3.17b}$$

$$\lambda\widetilde{i}(x)+\big(g(x)\widetilde{i}(x)\big)_x=-\big(\gamma(x)+\mu\big)\widetilde{i}(x), \tag{3.17c}$$

$$g(0)\widetilde{i}(0)=(\widetilde{S}+\sigma\widetilde{V})\int_0^\infty\beta(x)i^*(x)dx+(S^*+\sigma V^*)\int_0^\infty\beta(x)\widetilde{i}(x)dx. \tag{3.17d}$$

Solving the Eq. (3.17c) gives

$$\widetilde{i}(x)=\frac{g(0)\widetilde{i}(0)}{g(x)}e^{-\int_0^x\frac{\gamma(s)+\mu+\lambda}{g(s)}ds}. \tag{3.18}$$

Adding the Eqs. (3.17a) and (3.17b) together and plugging them into the Eq. (3.17d), we obtain

$$\begin{aligned}
g(0)\widetilde{i}(0)&=-(\lambda+\mu)(\widetilde{S}+\widetilde{V})\\
&=(\lambda+\mu)\left(\frac{S^*\int_0^\infty\beta(x)\widetilde{i}(x)dx}{\lambda+\mu+\varphi+\int_0^\infty\beta(x)i^*(x)dx}+\frac{\sigma V^*\int_0^\infty\beta(x)\widetilde{i}(x)dx-\varphi\widetilde{S}}{\lambda+\mu+\sigma\int_0^\infty\beta(x)i^*(x)dx}\right)\\
&=\left[S^*\left(\lambda+\mu+\sigma\int_0^\infty\beta(x)i^*(x)dx\right)+\sigma V^*\left(\lambda+\mu+\varphi+\int_0^\infty\beta(x)i^*(x)dx\right)+\varphi S^*\right]\\
&\quad\times\frac{(\lambda+\mu)\int_0^\infty\beta(x)\widetilde{i}(x)dx}{\left(\lambda+\mu+\varphi+\int_0^\infty\beta(x)i^*(x)dx\right)\left(\lambda+\mu+\sigma\int_0^\infty\beta(x)i^*(x)dx\right)}.
\end{aligned} \tag{3.19}$$

Then, taking Eqs. (3.10), (3.18) and dividing both sides of (3.19) by $g(0)\widetilde{i}(0)$, we have

$$\begin{aligned}
1=&\frac{S^*(\lambda+\mu)\int_0^\infty\beta(x)/g(x)e^{-\int_0^x\frac{\gamma(s)+\mu+\lambda}{g(s)}ds}dx}{\left(\lambda+\mu+\varphi+\int_0^\infty\beta(x)i^*(x)dx\right)\left(\lambda+\mu+\sigma\int_0^\infty\beta(x)i^*(x)dx\right)}\\
&\times\left(\left(\lambda+\mu+\sigma\int_0^\infty\beta(x)i^*(x)dx\right)+\frac{\sigma\varphi\left(\lambda+\mu+\varphi+\int_0^\infty\beta(x)i^*(x)dx\right)}{\mu+\sigma\int_0^\infty\beta(x)i^*(x)dx}+\varphi\right).
\end{aligned} \tag{3.20}$$

According to the Eq. (3.7b), Eq. (3.20) can be rewritten as

$$\begin{aligned}
&\left(\lambda+\mu+\varphi+\int_0^\infty\beta(x)i^*(x)dx\right)\left(\lambda+\mu+\sigma\int_0^\infty\beta(x)i^*(x)dx\right)\\
=&(\lambda+\mu)\int_0^\infty\frac{\beta(x)}{g(x)}e^{-\int_0^x\frac{\gamma(s)+\mu+\lambda}{g(s)}ds}dx\\
&\times\left(S^*\left(\lambda+\mu+\varphi+\sigma\int_0^\infty\beta(x)i^*(x)dx\right)+\sigma V^*\left(\lambda+\mu+\varphi+\int_0^\infty\beta(x)i^*(x)dx\right)\right).
\end{aligned} \tag{3.21}$$

Theorem 3.3. *The endemic equilibrium E^* is locally asymptotically stable when $\mathcal{R}_0 > 1$.*

Proof. Assuming $\lambda = \Re\lambda + \Im\lambda$ and $\Re\lambda \geq 0$, then the left side of the Eq. (3.21) gives

$$\begin{aligned}
&\sqrt{\left(\Re\lambda+\mu+\varphi+\int_0^\infty \beta(x)i^*(x)dx\right)^2+(\Im\lambda)^2} \\
&\quad\times\sqrt{\left(\Re\lambda+\mu+\sigma\int_0^\infty \beta(x)i^*(x)dx\right)^2+(\Im\lambda)^2} \\
&> \left|\lambda+\mu+\varphi+\int_0^\infty \beta(x)i^*(x)dx\right||\lambda+\mu|. \qquad (3.22)
\end{aligned}$$

However, by the Eq. (3.7d), the right side of (3.21) yields

$$\begin{aligned}
&\left(S^*\left(\lambda+\mu+\varphi+\sigma\int_0^\infty \beta(x)i^*(x)dx\right)+\sigma V^*\left(\lambda+\mu+\varphi+\int_0^\infty \beta(x)i^*(x)dx\right)\right) \\
&\quad\times(\lambda+\mu)\int_0^\infty \frac{\beta(x)}{g(x)}e^{-\int_0^x \frac{\gamma(s)+\mu+\lambda}{g(s)}ds}dx \\
&\leq \left|(S^*+\sigma V^*)\int_0^\infty \frac{\beta(x)}{g(x)}e^{-\int_0^x \frac{\gamma(s)+\mu}{g(s)}ds}dx\right|\left|\lambda+\mu+\varphi+\int_0^\infty \beta(x)i^*(x)dx\right||\lambda+\mu| \\
&= \left|\lambda+\mu+\varphi+\int_0^\infty \beta(x)i^*(x)dx\right||\lambda+\mu|.
\end{aligned}$$

That is to say, if $\Re\lambda \geq 0$, Eq. (3.21) is invalid. Hence, the real parts of the solutions to the characteristic equation (3.21) must be negative and E^* is locally asymptotically stable. □

4 An optimal control problem

Two primary interventions aimed at mitigating the transmission scale of influenza A are antiviral treatment and vaccination. The former control can prevent IAV from producing new virus particles, while the latter one can reduce the activity of IAV. In this study, we compare the effects of these control strategies to identify the optimal approach. Let $u_1(\cdot)$ quantify the therapeutic intervention efficacy on viral replication kinetics, and $u_2(\cdot)$ denote the control measures that reduce the probability of host-to-host transmission. The coupled systems of influenza model with these two control measures are then formulated as follows:

$$\frac{dP(x)}{dx} = r_p\big(1-u_1(x)\big)P(x)\left(1-\frac{P(x)}{K_p}\right)-C_pP(x)E(x), \qquad (4.1a)$$

$$\frac{dE(x)}{dx} = \frac{\beta_e E(x)P(x)}{P(x)+K_e}-C_eE(x)+S_e, \qquad (4.1b)$$

$$\frac{dS(t)}{dt}=\Lambda-\varphi\big(1+u_2(t)\big)S(t)-S(t)\int_0^\infty\beta(x)i(x,t)dx-\mu S(t), \tag{4.1c}$$

$$\frac{dV(t)}{dt}=\varphi\big(1+u_2(t)\big)S(t)-\sigma V(t)\int_0^\infty\beta(x)i(x,t)dx-\mu V(t), \tag{4.1d}$$

$$i_t(x,t)+\big(g(x)i(x,t)\big)_x=-\big(\gamma(x)+\mu\big)i(x,t), \tag{4.1e}$$

$$g(0)i(0,t)=S(t)\int_0^\infty\beta(x)i(x,t)dx+\sigma V(t)\int_0^\infty\beta(x)i(x,t)dx, \tag{4.1f}$$

$$\frac{dR(t)}{dt}=\int_0^\infty\gamma(x)i(x,t)dx-\mu R(t). \tag{4.1g}$$

We define the control admissible set as

$$U=\big\{(u_1,u_2)\in L^\infty(0,\bar{x})\times L^\infty(0,\bar{t})\mid 0\le u_i\le\bar{u}_i,i=1,2\big\},$$

where $\bar{u}_i$ $(i=1,2)$ are positive constants, $\bar{x}$ denotes the final control age-since-infection and $\bar{t}$ represents the final control time. We aim to mitigate the propagation of IAV under resource-constrained conditions. Therefore, we establish the objective function as below

$$\begin{aligned}J(u_1,u_2)=&\int_0^{\bar{x}}\left[A_1P(x)+A_2u_1(x)P(x)+\frac{1}{2}B_1u_1^2(x)\right]dx\\&+\int_0^{\bar{t}}\left[A_3u_2(t)S(t)+\frac{1}{2}B_2u_2^2(t)+A_4\int_0^{\bar{x}}i(x,t)dx\right]dt,\end{aligned} \tag{4.2}$$

where A_m $(m=1,2,3,4)$ represent the weight coefficients and $B_n(n=1,2)$ represent the cost of implementing the controls. The units of A_1 and A_2 are given in RMB per viral copies per milliliter (RMB/copies/mL). The units of A_3 and A_4 are given in RMB per person (RMB/person). Both B_1 and B_2 are expressed in RMB. The optimal control problem involves finding the admissible pair $(u_1^*,u_2^*)\in U$ that minimizes the objective function value in (4.2), i.e.

$$J(u_1^*,u_2^*)=\min_{u_1,u_2\in U}J(u_1,u_2).$$

In what follows, we need to analyze the sensitivity system, derive the adjoint system, and determine the optimal controls. Let y_j $(j=1,\dots,5)$ denote the sensitivities for the state variables P,E,S,V, and i, respectively. Substituting $u_i^*=u_i+\varepsilon l_i$ $(i=1,2)$ into system (4.1) to find the derivative in ε and set $\varepsilon=0$, we have the following sensitivity system:

$$\begin{aligned}y_1'(x)=&r_p\big(1-u_1(x)\big)\left(y_1(x)-2P(x)\frac{y_1(x)}{K_p}\right)-r_pl_1P(x)\left(1-\frac{P(x)}{K_p}\right)\\&-C_p\big(y_1(x)E(x)+P(x)y_2(x)\big),\end{aligned} \tag{4.3a}$$

$$y_2'(x)=\frac{\beta_e\big(y_2(x)P(x)+E(x)y_1(x)\big)\big(P(x)+K_e\big)-\beta_eE(x)P(x)y_1(x)}{\big(P(x)+K_e\big)^2}-C_ey_2(x), \tag{4.3b}$$

$$y_3'(t) = -\varphi l_2 S(t) - \varphi\big(1+u_2(t)\big)y_3(t) - y_3(t)\int_0^\infty \beta(x)i(x,t)dx$$
$$-S(t)\int_0^\infty \big(\beta y_1(t)i(x,t)+\beta(x)y_5(x,t)\big)dx - \mu y_3(t), \tag{4.3c}$$
$$y_4'(t) = \varphi l_2 S(t) + \varphi\big(1+u_2(t)\big)y_3(t) - \sigma y_4(t)\int_0^\infty \beta(x)i(x,t)dx$$
$$-\sigma V(t)\int_0^\infty \big(\beta y_1(x)i(x,t)+\beta(x)y_5(x,t)\big)dx - \mu y_4(t), \tag{4.3d}$$
$$\frac{dy_5(x,t)}{dt} + \frac{d\big(g(x)y_5(x,t)\big)}{dx} = -\gamma y_2(x)i(x,t) - \big(\gamma(x)+\mu\big)y_5(x,t), \tag{4.3e}$$
$$g(0)y_5(0,t) = \big(y_3(t)+\sigma y_4(t)\big)\int_0^\infty \beta(x)i(x,t)dx$$
$$+\big(S(t)+\sigma V(t)\big)\int_0^\infty \big(\beta y_1(x)i(x,t)+\beta(x)y_5(x,t)\big)dx, \tag{4.3f}$$

where the initial conditions are given by

$$y_j(0)=0, \quad j=1,2,3,4, \quad y_5(x,0)=0, \quad x\in(0,\bar{x}).$$

The payoff function satisfies

$$\frac{dJ}{d\varepsilon}\Big|_{\varepsilon=0} = \int_0^{\bar{x}} [A_1 y_1(x) + A_2 l_1 P(x) + A_2 u_1(x) y_1(x) + B_1 l_1 u_1(x)]dx$$
$$+\int_0^{\bar{t}} \left[A_3 l_2 S(t) + A_3 u_2(t) y_3(t) + B_2 l_2 u_2(t) + A_4 \int_0^{\bar{x}} y_5(x,t)dx\right] dt.$$

Lemma 4.1. *Let q,η,ξ,c, and m represent the adjoint variables for P,E,S,V, and i, correspondingly. For $(u_1,u_2)\in U$, the adjoint system for system* (4.3) *is given by*

$$-q'(x) = q(x)\left(r_p\big(1-u_1(x)\big)\left(1-\frac{2P(x)}{K_p}\right) - C_p E(x)\right) + \eta(x)\left(\frac{\beta_e E(x) K_e}{(P(x)+K_e)^2}\right) \tag{4.4a}$$
$$-\int_0^{\bar{t}} \big(\xi(t)S(t) + c(t)\sigma V(t) - m(0,t)\big(S(t)+\sigma V(t)\big)\big)\beta i(x,t)dt + A_1 + A_2 u_1(x),$$
$$-\eta'(x) = -q(x)C_p P(x) + \eta(x)\left(\frac{\beta_e P(x)}{P(x)+K_e} - C_e\right) - \int_0^{\bar{t}} \gamma m(x,t)i(x,t)dt, \tag{4.4b}$$
$$-\xi'(t) = -\xi(t)\left(\varphi\big(1+u_2(t)\big) + \int_0^{\bar{x}} \beta(x)i(x,t)dx + \mu\right) + c(t)\big(\varphi\big(1+u_2(t)\big)\big)$$
$$+m(0,t)\int_0^{\bar{x}} \beta(x)i(x,t)dx + A_3 u_2(t), \tag{4.4c}$$
$$-c'(t) = -c(t)\left(\sigma\int_0^{\bar{x}} \beta(x)i(x,t)dx + \mu\right) + m(0,t)\sigma\int_0^{\bar{x}} \beta(x)i(x,t)dx, \tag{4.4d}$$

$$-m_t(x,t)-g(x)m_x(x,t)=-\big(\xi(t)S(t)+c(t)\sigma V(t)-m(0,t)\big(S(t)+\sigma V(t)\big)\big)\beta(x)$$
$$-m(x,t)(\gamma(x)+\mu)+A_4, \tag{4.4e}$$

where the transversality conditions of adjoint variables are taken by

$$\begin{aligned} &q(\bar{x})=\eta(\bar{x})=\xi(\bar{t})=c(\bar{t})=0, \quad m(x,\bar{t})=0, \quad x\in(0,\bar{x})\\ &m(\bar{x},t)=0, \qquad\qquad\qquad\qquad\quad t\in(0,\bar{t}). \end{aligned}$$

Proof. Dividing the sensitivity equations in (4.3) into three operators $\mathcal{L}_1,\mathcal{L}_2$ and $\mathcal{L}_3$, we obtain

$$\mathcal{L}_1\begin{pmatrix}y_1\\y_2\end{pmatrix}=\begin{pmatrix}-r_pl_1P(x)\left(1-\dfrac{P(x)}{K_p}\right)\\0\end{pmatrix}, \quad \mathcal{L}_2\begin{pmatrix}y_3\\y_4\end{pmatrix}=\begin{pmatrix}-\varphi l_2S(t)\\\varphi l_2S(t)\end{pmatrix}, \quad \mathcal{L}_3y_5(x,t)=0.$$

Then, define the operators $\mathcal{L}_2^*,\mathcal{L}_2^*$ and $\mathcal{L}_3^*$ to satisfy

$$\begin{aligned} &\int_0^{\bar{x}}(q,\eta)\mathcal{L}_1(y_1,y_2)dx+\int_0^{\bar{t}}(\xi,c)\mathcal{L}_2(y_3,y_4)dt+\int_0^{\bar{t}}\int_0^{\bar{x}}m\mathcal{L}_3y_5dxdt\\ =&\int_0^{\bar{x}}(y_1,y_2)\mathcal{L}_1^*(q,\eta)dx+\int_0^{\bar{t}}(y_3,y_4)\mathcal{L}_2^*(\xi,c)dt+\int_0^{\bar{t}}\int_0^{\bar{x}}y_5\mathcal{L}_3^*mdxdt \end{aligned}$$

with the adjoint equations

$$\mathcal{L}_1^*\begin{pmatrix}q\\\eta\end{pmatrix}=\begin{pmatrix}A_1+A_2u_1\\0\end{pmatrix}, \quad \mathcal{L}_2^*\begin{pmatrix}\xi\\c\end{pmatrix}=\begin{pmatrix}A_3u_2\\0\end{pmatrix}, \quad \mathcal{L}_3^*m=A_4.$$

Thus, we can derive the adjoint equations from the relationship between such operators

$$\int_0^{\bar{x}}q(x)y_1'(x)dx=\int_0^{\bar{x}}q(x)d\big(y_1(x)\big)=q(\bar{x})y_1(\bar{x})-q(0)y_1(0)-\int_0^{\bar{x}}y_1(x)q'(x)dx.$$

That is,

$$\begin{aligned} &-\int_0^{\bar{x}}y_1(x)q'(x)dx\\ =&\int_0^{\bar{x}}q(x)\left(r_p(1-u_1)y_1\left(1-\frac{2P}{K_p}\right)-r_pl_1P\left(1-\frac{P}{K_p}\right)-C_p(y_1E+Py_2)\right)dx. \end{aligned}$$

Likewise, we have

$$-\int_0^{\bar{x}}y_2(x)\eta'(x)dx=\int_0^{\bar{x}}\eta(x)\left(\frac{\beta_e(y_2P+Ey_1)(P+K_e)-\beta_eEPy_1}{(P+K_e)^2}-C_ey_2\right)dx,$$

and

$$\begin{aligned}
&\int_0^{\bar{x}}\int_0^{\bar{t}} m(x,t)\left(\frac{dy_5(x,t)}{dt}+\frac{d\big(g(x)y_5(x,t)\big)}{dx}\right)dtdx\\
&=\int_0^{\bar{x}}\int_0^{\bar{t}} m\frac{dy_5(x,t)}{dt}dtdx+\int_0^{\bar{x}}\int_0^{\bar{t}} m\frac{d\big(g(x)y_5(x,t)\big)}{dx}dtdx\\
&=\int_0^{\bar{x}}\int_0^{\bar{t}} md\big(y_5(x,t)\big)dx+\int_0^{\bar{t}}\int_0^{\bar{x}} md\big(g(x)y_5(x,t)\big)dt\\
&=\int_0^{\bar{x}}\left(m(x,\bar{t})y_5(x,\bar{t})-m(x,0)y_5(x,0)-\int_0^{\bar{t}} y_5(x,t)d\big(m(x,t)\big)\right)dx\\
&\quad+\int_0^{\bar{t}}\left(m(\bar{x},t)g(\bar{x})y_5(\bar{x},t)-m(0,t)g(0)y_5(0,t)-\int_0^{\bar{x}} g(x)y_5(x,t)d\big(m(x,t)\big)\right)dt.
\end{aligned}$$

Hence,

$$\begin{aligned}
&-\int_0^{\bar{t}}\int_0^{\bar{x}} y_5(x,t)\big(m_t(x,t)+g(x)m_x(x,t)\big)dxdt\\
&=\int_0^{\bar{t}} m(0,t)\left(\big(y_3(t)+\sigma y_4(t)\big)\int_0^{\bar{x}}\beta(x)i(x,t)dx\right)dt\\
&\quad+\int_0^{\bar{t}} m(0,t)\left(\big(S(t)+\sigma V(t)\big)\int_0^{\bar{x}}\big(\beta y_1(t)i(x,t)+\beta(x)y_5(x,t)\big)dx\right)dt\\
&\quad+\int_0^{\bar{t}}\int_0^{\bar{x}} m(x,t)\big(-\gamma y_2(x)i(x,t)-\big(\gamma(x)+\mu\big)y_5(x,t)\big)dxdt.
\end{aligned}$$

By organizing the equations according to how the sensitivity and adjoint operators are connected, we obtain the adjoint system (4.4). □

Lemma 4.2. *Let* (P^*,E^*,S^*,V^*,i^*) *and* (q,η,ξ,c,m) *be the solutions of systems* (4.1) *and* (4.4)*, then the optimal controls* $(u_1^*,u_2^*)\in U$ *is characterized by*

$$\begin{aligned}
u_1^*(x)&=K_1\left(\frac{q(x)r_pP^*(x)\big(1-P^*(x)/K_p\big)-A_2P^*(x)}{B_1}\right),\\
u_2^*(t)&=K_2\left(\frac{\big(\big(\xi(t)-c(t)\big)\varphi-A_3\big)S^*(t)}{B_2}\right),
\end{aligned}\tag{4.5}$$

where

$$K_i(y)=\begin{cases}0, & y<0,\\ y, & 0\le y\le \bar{u}_i,\\ \bar{u}_i, & y>\bar{u}_i,\end{cases}\quad i=1,2.$$

Proof. If $(u_1^*,u_2^*)\in U$ is a pair of optimal controls minimizing the payoff function (4.2), then we get

$$
\begin{aligned}
0\leq & \lim_{\epsilon\to 0^+}\frac{J\left(u_1^\epsilon,u_2^\epsilon\right)-J(u_1^*,u_2^*)}{\epsilon} \quad \left(u_i^\epsilon=u_i^*+\epsilon l_i\right)\\
=&\lim_{\epsilon\to 0^+}\int_0^{\bar{x}}A_1\frac{P^\epsilon-P^*}{\epsilon}dx+\lim_{\epsilon\to 0^+}\int_0^{\bar{t}}\int_0^{\bar{x}}A_4\frac{i^\epsilon-i^*}{\epsilon}dxdt\\
&+\lim_{\epsilon\to 0^+}\int_0^{\bar{x}}\frac{B_1\left(u_1^\epsilon-u_1^*\right)\left(u_1^\epsilon+u_1^*\right)}{\epsilon}dx+\lim_{\epsilon\to 0^+}\int_0^{\bar{t}}\frac{B_2\left(u_2^\epsilon-u_2^*\right)\left(u_2^\epsilon+u_2^*\right)}{\epsilon}dt\\
&+\lim_{\epsilon\to 0^+}\int_0^{\bar{x}}A_2\left[\frac{u_1^\epsilon(P^\epsilon-P^*)}{\epsilon}+\frac{P^*\left(u_1^\epsilon-u_1^*\right)}{\epsilon}\right]dx\\
&+\lim_{\epsilon\to 0^+}\int_0^{\bar{t}}A_3\left[\frac{u_2^\epsilon(S^\epsilon-S^*)}{\epsilon}+\frac{S^*\left(u_2^\epsilon-u_2^*\right)}{\epsilon}\right]dt\\
=&\int_0^{\bar{x}}A_1y_1(x)dx+\int_0^{\bar{t}}\int_0^{\bar{x}}A_4y_5(x,t)dxdt+2\int_0^{\bar{x}}B_1u_1^*(x)l_1(x)dx+2\int_0^{\bar{t}}B_2u_2^*(t)l_2(t)dt\\
&+\int_0^{\bar{x}}\left(A_2y_1(x)u_1^*(x)+A_2P^*(x)l_1(x)\right)dx+\int_0^{\bar{t}}\left(A_3y_3(t)u_2^*(t)+A_3S^*(t)l_2(t)\right)dt\\
=&\int_0^{\bar{x}}(y_1,y_2)\begin{bmatrix}A_1+A_2u_1\\0\end{bmatrix}dx+\int_0^{\bar{t}}(y_3,y_4)\begin{bmatrix}A_3u_2\\0\end{bmatrix}dt+\int_0^{\bar{t}}\int_0^{\bar{x}}A_4y_5(x,t)dxdt\\
&+2\int_0^{\bar{x}}B_1u_1^*(x)l_1(x)dx+2\int_0^{\bar{t}}B_2u_2^*(t)l_2(t)dt+\int_0^{\bar{x}}A_2P^*(x)l_1(x)dx\\
&+\int_0^{\bar{t}}A_3S^*(t)l_2(t)dt.
\end{aligned}
\tag{4.6}
$$

Using the adjoint system (4.4) and the relationship between sensitivity and operators, we obtain

$$
\begin{aligned}
&\int_0^{\bar{x}}(y_1,y_2)\begin{bmatrix}A_1+A_2u_1\\0\end{bmatrix}dx+\int_0^{\bar{t}}(y_3,y_4)\begin{bmatrix}A_3u_2\\0\end{bmatrix}dt+\int_0^{\bar{t}}\int_0^{\bar{x}}A_4y_5(x,t)dxdt\\
=&\int_0^{\bar{x}}y_1\Bigg[-q'(x)-q(x)\left(r_p\left(1-u_1(x)\right)\left(1-\frac{2P(x)}{K_p}\right)-C_pE(x)\right)-\eta(x)\left(\frac{\beta_eE(x)K_e}{\left(P(x)+K_e\right)^2}\right)\\
&\qquad+\int_0^{\bar{t}}\left(\xi(t)S(t)+c(t)\sigma V(t)-m(0,t)\left(S(t)+\sigma V(t)\right)\right)\beta i(x,t)dt\Bigg]dx\\
&+\int_0^{\bar{x}}y_2(x)\left[-\eta'(x)+q(x)C_pP(x)-\eta(x)\left(\frac{\beta_eP(x)}{P(x)+K_e}-C_e\right)+\int_0^{\bar{t}}\gamma m(x,t)i(x,t)dt\right]dx\\
&+\int_0^{\bar{t}}y_3(t)\left[-\xi'(t)+\xi(t)\left(\varphi\left(1+u_2(t)\right)+\int_0^{\bar{x}}\beta(x)i(x,t)dx+\mu\right)-c\left(\varphi\left(1+u_2(t)\right)\right)\right]dt\\
&-\int_0^{\bar{t}}\int_0^{\bar{x}}y_3(t)m(0,t)\beta(x)i(x,t)dxdt+\int_0^{\bar{t}}y_4(t)\left[-c'(t)+c(t)\left(\sigma\int_0^{\bar{x}}\beta(x)i(x,t)dx+\mu\right)\right]dt
\end{aligned}
$$

$$
\begin{aligned}
&-\int_0^{\bar{t}}\int_0^{\bar{x}} y_4(t)m(0,t)\sigma\beta(x)i(x,t)dxdt+\int_0^{\bar{t}}\int_0^{\bar{x}} y_5(x,t)\big(-m_t(x,t)-g(x)m_x(x,t)\big)dxdt\\
&+\int_0^{\bar{t}}\int_0^{\bar{x}} y_5(x,t)\big[\big(\xi(t)S(t)+c(t)\sigma V(t)-m(0,t)\big(S(t)+\sigma V(t)\big)\big)\beta(x)\\
&\qquad\qquad +m(x,t)(\gamma(x)+\mu)\big]dxdt.
\end{aligned}
$$

For notational simplicity, we temporarily omit the asterisks. By substituting the sensitivity system (4.3) and the transversality conditions (4.4) into above equation, and applying standard optimal control techniques, we can derive the characteristic expression of $(u_1^*,u_2^*)\in U$, as presented in Eq. (4.5). □

5 Numerical simulations

In this section, we use the forward and backward sweep algorithms to numerically analyze the state and adjoint systems. For convenience, the rectangular area $[0,\bar{x}]\times[0,\bar{t}]$ is discretized with the step size Δx and Δt in the immune state-time space. Let

$$
\begin{aligned}
&t_n=n\Delta t,\quad n=1,\dots,N,\\
&x_j=j\Delta x,\quad j=1,\dots,M.
\end{aligned}
$$

Accordingly, we get a discretization of system (4.1) as

$$
\begin{aligned}
&\frac{P_j-P_{j-1}}{\Delta x}=r_p\big(1-u_1(x)\big)P_{j-1}\left(1-\frac{P_{j-1}}{K_p}\right)-C_pP_jE_{j-1},\\
&\frac{E_j-E_{j-1}}{\Delta x}=\frac{\beta_eE_{j-1}P_j}{P_j+K_e}-C_eE_j+S_e,\\
&\frac{S^n-S^{n-1}}{\Delta t}=\Lambda-\varphi\big(1+u_2^n\big)S^n-S^n\sum_{j=1}^{M}\beta P_ji_j^{n-1}\Delta x-\mu S^n,\\
&\frac{V^n-V^{n-1}}{\Delta t}=\varphi\big(1+u_2^n\big)S^n-\sigma V^n\sum_{j=1}^{M}\beta P_ji_j^{n-1}\Delta x-\mu V^n,\\
&\frac{i_j^n-i_j^{n-1}}{\Delta t}+\frac{g_ji_j^n-g_{j-1}i_{j-1}^n}{\Delta x}=-(\gamma E_j+\mu)i_j^n,
\end{aligned}
\tag{5.1}
$$

where

$$
g_1i_1^n=(S^n+\sigma V^n)\sum_{j=1}^{M}\beta P_ji_j^n\Delta x.
$$

Solving system (5.1) yields

$$
P_j=\frac{P_{j-1}+\Delta x\big(r_p(1-u_{1_j})P_{j-1}(1-P_{j-1}/K_p)\big)}{1+\Delta xC_pE_{j-1}},
$$

$$
\begin{aligned}
E_j &= \frac{E_{j-1}+\Delta x\big((\beta_e E_{j-1}P_j)/(P_j+K_e)+S_e\big)}{1+\Delta x C_e},\\
S^n &= \frac{S^{n-1}+\Delta t\Lambda}{1+\Delta t\big(\varphi\big(1+u_2^n\big)+\sum_{j=1}^{M}\beta P_j i_j^{n-1}\Delta x+\mu\big)},\\
V^n &= \frac{V^{n-1}+\Delta t\big(\varphi\big(1+u_2^n\big)S^n\big)}{1+\Delta t\big(\sigma\sum_{j=1}^{M}\beta P_j i_j^{n-1}\Delta x+\mu\big)},\\
i_j^n &= \frac{i_j^{n-1}+\Delta t\big(g_{j-1}i_{j-1}^n/\Delta x\big)}{1+\Delta t(g_j/\Delta x+\gamma E_j+\mu)}.
\end{aligned}
$$

The difference format of system (4.4) is given by

$$
\begin{aligned}
-\frac{q_{j+1}-q_j}{\Delta x} &= q_{j+1}\left(r_p(1-u_{1_{j+1}})\left(1-\frac{2P_j}{K_p}\right)-C_pE_j\right)+\eta_{j+1}\frac{\beta_e E_j K_e}{(P_j+K_e)^2}+A_1+A_2u_{1_{j+1}}\\
&\quad-\sum_{n=1}^{N}\big(\xi^{n+1}S^n+c^{n+1}\sigma V^n-m_1^{n+1}(S^n+\sigma V^n)\big)\beta i_j^n\Delta t,\\
-\frac{\eta_{j+1}-\eta_j}{\Delta x} &= -q_jC_pP_j+\eta_{j+1}\left(\frac{\beta_eP_j}{P_j+K_e}-C_e\right)-\sum_{n=1}^{N}\gamma m_{j+1}^n i_{j+1}^n\Delta t,\\
-\frac{\xi^{n+1}-\xi^n}{\Delta t} &= -\xi^n\left(\varphi\big(1+u_2^{n+1}\big)+\sum_{j=1}^{M}\beta P_j i_j^n\Delta x+\mu\right)+c^{n+1}\big(\varphi\big(1+u_2^{n+1}\big)\big)\\
&\quad+m_1^{n+1}\sum_{j=1}^{M}\beta P_j i_j^n\Delta x+A_3u_2^n,\\
-\frac{c^{n+1}-c^n}{\Delta t} &= -c^n\left(\sigma\sum_{j=1}^{M}\beta P_j i_j^n\Delta x+\mu\right)+m_1^{n+1}\sigma\sum_{j=1}^{M}\beta P_j i_j^n\Delta x,\\
-\frac{m_j^{n+1}-m_j^n}{\Delta t}-g_j\frac{m_{j+1}^n-m_j^n}{\Delta x} &= -\big(\xi^nS^n+c^n\sigma V^n-m_1^{n+1}(S^n+\sigma V^n)\big)\beta P_j\\
&\quad-m_j^n(\gamma E_j+\mu)+A_4.
\end{aligned}
\tag{5.2}
$$

Solving system (5.2) gives

$$
\begin{aligned}
q_j &= q_{j+1}+\Delta x\left[q_{j+1}\left(r_p(1-u_{1_{j+1}})\left(1-\frac{2P_j}{K_p}\right)-C_pE_j\right)+\eta_{j+1}\frac{\beta_eE_jK_e}{(P_j+K_e)^2}\right.\\
&\quad\left.-\sum_{n=1}^{N}\big(\xi^{n+1}S^n+c^{n+1}\sigma V^n-m_1^{n+1}(S^n+\sigma V^n)\big)\beta i_j^n\Delta t+A_1+A_2u_{1_{j+1}}\right],\\
\eta_j &= \eta_{j+1}+\Delta x\left[\eta_{j+1}\left(\frac{\beta_eP_j}{P_j+K_e}-C_e\right)-q_jC_pP_j-\sum_{n=1}^{N}\gamma m_{j+1}^n i_{j+1}^n\Delta t\right],
\end{aligned}
$$

$$\xi^n = \frac{\xi^{n+1} + \Delta t\left(c^{n+1}\varphi\left(1+u_2^{n+1}\right) + m_1^{n+1}\sum_{j=1}^{M}\beta P_j i_j^n \Delta x + A_3 u_2^{n+1}\right)}{1+\Delta t\left(\varphi\left(1+u_2^{n+1}\right) + \sum_{j=1}^{M}\beta P_j i_j^n \Delta x + \mu\right)},$$

$$c^n = \frac{c^{n+1} + \Delta t\left(m_1^{n+1}\sigma\sum_{j=1}^{M}\beta P_j i_j^n \Delta x\right)}{1+\Delta t\left(\sigma\sum_{j=1}^{M}\beta P_j i_j^n \Delta x + \mu\right)},$$

$$m_j^n = \frac{m_j^{n+1} + \Delta t\left(g_j m_{j+1}^n/\Delta x - \left(\xi^n S^n + c^n\sigma V^n - m_1^{n+1}(S^n+\sigma V^n)\right)\beta P_j + A_4\right)}{1+\Delta t(g_j/\Delta x + \gamma E_j + \mu)}.$$

Now, we apply forward and backward iterative finite difference schemes to Eqs. (5.1) and (5.2), respectively, using the following uptake rules:

$$u_{1_j} = \frac{q_j r_p P_j(1-P_j/K_p) - A_2 P_j}{B_1}, \quad u_2^n = \frac{(\xi^n - c^n)\varphi S^n - A_3 S^n}{B_2}.$$

In the end, the control variables are updated by the following forms:

$$u_{1_j}^* = \min\left\{\max\{0, u_{1_j}\}, \bar{u}_1\right\}, \quad u_2^{n*} = \min\left\{\max\left\{0, u_2^n\right\}, \bar{u}_2\right\}.$$

At last, the finite difference program continues until the error is within an acceptable range.

Given the limited resources for implementing control measures, it is essential to evaluate the cost and effectiveness of each strategy in order to determine the most suitable control for reducing the risk of disease transmission. In what follows, we consider four strategies and compare their outcomes:

(A) Without control.
(B) Only implementing antiviral treatment, that is, control u_1 is on, and control u_2 is off.
(C) Only taking vaccination, that is, control u_2 is on, and control u_1 is off.
(D) Implementing both antiviral treatment and vaccination.

From Fig. 1, we observe that coupled controls result in a rapid decline in virus concentration initially, maintaining it at a low level, while antiviral treatment is slightly less effective. Strategy C, on the other hand, shows a slower decline in virus concentration, suggesting that vaccination takes more time to control the spread of IAV. Regarding the number of infected individuals, both strategies B and D reduce infections, though with differing effectiveness. Strategy D leads to a significant reduction in infections, with numbers dropping quickly and remaining low for a broad period. In contrast, vaccination (strategy C) has the weakest effect, with a slower decline in infections that becomes more noticeable over time. In terms of public health, the effectiveness of the strategies follows this order: D > B > C > A.

Figs. 1(c) and 1(d) show the optimal control intensities for each strategy. In strategy B, antiviral treatment intensity is adjusted according to changes in age-since-infection, showing a negative correlation. In strategy C, the vaccination intensity starts high and

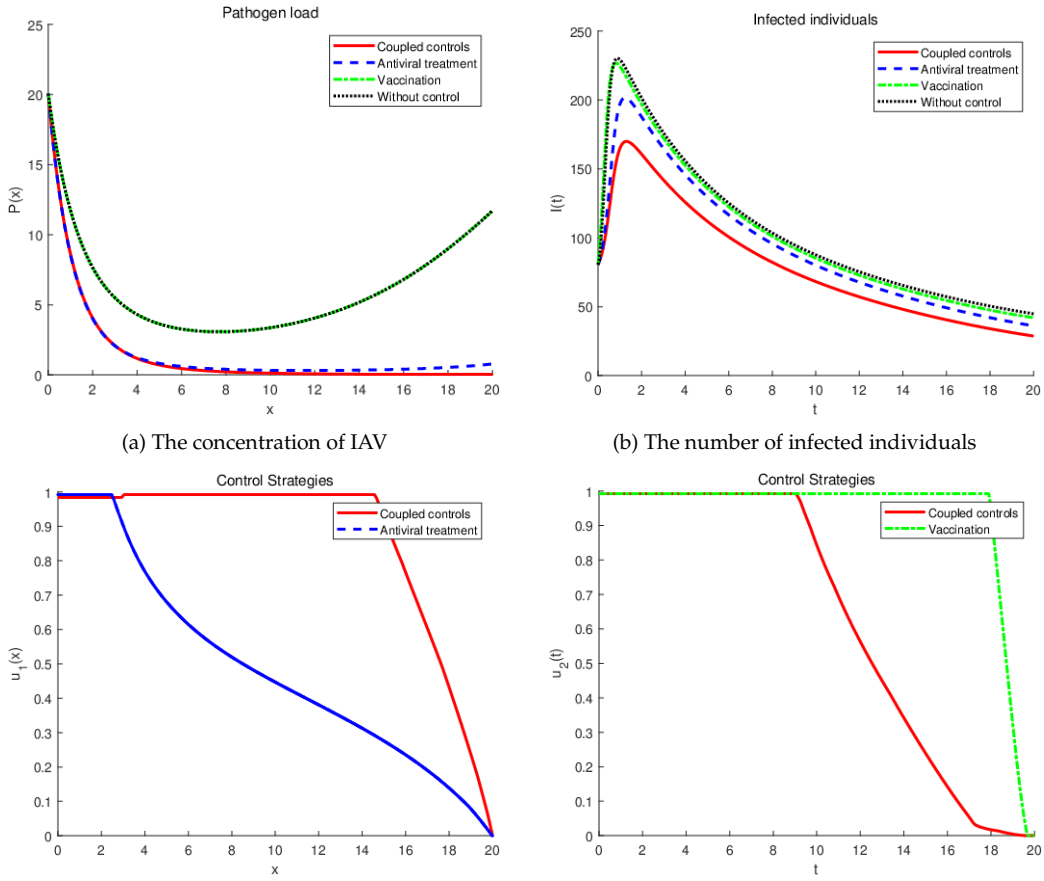

(a) The concentration of IAV

(b) The number of infected individuals

(c) Optimal intensity of antiviral treatment

(d) Optimal intensity of vaccination

Figure 1: The concentration of IAV and the number of infected individuals with implementing strategies (1)-(4), and the optimal intensity of $u_1(x)$ and $u_2(t)$ under strategies (1)-(3), where $g(x)=e^{-0.05x}$, $\beta=0.02$, $\gamma=0.06$, $\mu=0.02$.

remains elevated for a longer period. Strategy D maintains both antiviral treatment and vaccination at relatively high levels for a longer time.

Next, we take into account the implementation costs of the measures in our decision-making process through a cost-effectiveness analysis. This analysis includes three key indicators: total cost, reduced infections and the incremental cost-effectiveness ratio (ICER), which is calculated by dividing the cost difference by the number of infections prevented [1]. Below, we present the overall expenses for each strategy

$$\text{Total cost}=\int_0^{\bar{x}} A_2u_1(x)P(x)dx+\int_0^{\bar{t}} A_3u_2(t)S(t)dt.$$

For comparison, we fixed parameters A_1=10, A_2=5, A_3=2, A_4=10, B_1=10, and B_2=10. Table 1 presents the three key metrics for cost-effectiveness analysis. From Table 1, we

observe that the total cases decrease in the order $A > C > B > D$. Observing the second column of Table 1, the research findings show that coupled controls result in the highest number of avoided influenza cases, although they also incur the highest total cost. As observed in the last column, strategy B has the lowest ICER, suggesting that antiviral treatment offers the best cost-effectiveness.

$$\text{ICER}[(\text{B})(\text{C})] = \frac{9.3579 - 169.7580}{15.7913 - 3.6339} = -13.1936.$$

According to the above value of ICER, the implementation of antiviral treatment saves 13.19 RMB per person compared to vaccination. The cost of vaccination exceeds that of antiviral treatment.

The key to determining the best control strategy lies in finding the balance between its effectiveness and cost. To evaluate the cost-effectiveness of each approach, it is essential to consider not only the extent of influenza control but also the costs involved in implementing these strategies. Next, we perform a cost-benefit analysis at three different cost levels:

1. Low cost ($A_2 = 5, A_3 = 2$).
2. Moderate cost ($A_2 = 50, A_3 = 20$).
3. High cost ($A_2 = 500, A_3 = 200$).

Fixed weight coefficients are set as $B_1 = 300$ and $B_2 = 200$. We aim to explore how varying cost levels affect the magnitude of influenza spread. Table 2 indicates that the objective function values increase as control costs rise, while the total number of cases

Table 1: The number of influenza cases, overall expenses and ICER under strategies A-D.

Strategies	Total cases	Reduced infection	Overall expenses	ICER
A (Without control)	230.2602	–	–	–
B (Antiviral treatment)	214.4689	15.7913	9.3579	0.5925
C (Vaccination)	226.6263	3.6339	169.7580	46.7150
D (Coupled controls)	169.3916	60.8686	235.8851	3.8753

Table 2: The influenza infection scenarios under different cost levels B-D.

Cost level	Antiviral treatment		Vaccination		Combined controls	
	IS	OFV	IS	OFV	IS	OFV
Low cost	201.5163	3521	226.7568	423320	169.9426	293810
Moderate cost	201.5352	3640	226.7568	425850	169.9323	296660
High cost	209.4329	4738	226.5611	448830	169.0362	317570
IS: The number of infected individuals at different cost levels under strategies B-D. OFV: The objective function values at different cost levels under strategies B-D.						

shows only a slight reduction, except for strategy B. Specifically, influenza cases increase by 3.94% with the application of antiviral treatment, and the objective function rises by 34.55% as the cost moves from low to high. Additionally, the objective function value for coupled controls and vaccination increase by approximately 8.06% and 6.04%, respectively. According to Table 2, we see that antiviral treatment results in the lowest value for the objective function, while combined treatment minimizes the number of infected individuals.

6 Discussion

We proposed a multi-scale epidemiological model for influenza according to previous studies [17, 28]. The connection mechanisms between within-host and between-host dynamics are assumed to involve the spread and recovery rates of IAV, as well as the sizes of CTLs. We used a size-structured model to capture the interaction between these two scales. The purpose of our research is to explore the complex dynamics of IAV and the immune system in the coupled models and to gain insight of how the viral load of individuals affects the progression of influenza.

Theoretically, we derived the reproduction numbers for both systems involved and investigated the dynamics of each equilibrium. Specifically, for the infection-free equilibrium, influenza will be eliminated if $\mathcal{R}_0 < 1$ and will persist conversely. If there exists an endemic equilibrium, i.e. $\mathcal{R}_0 > 1$, it must be locally asymptotically stable. Then, we set an optimal control system for influenza and provided a detailed derivation procedure for the adjoint system. Finally, we acquired the expression for a pair of optimal controls.

Numerically, we obtained time series diagrams under four scenarios using finite difference method. The numerical results indicated that the combined effect of antiviral treatment and vaccination is the most effective strategy when focusing solely on public health. However, considering the limitations in total costs for these measures, an analysis of ICER for the four strategies revealed that antiviral treatment is the most cost-effective option. Based on the cost-benefit analysis at three cost levels, we found that the high-cost coupled controls are the best choice for slowing down the spread of influenza. While increasing expenditure does not significantly reduce the number of influenza cases, it results in a substantial increase in the objective function value. Consequently, low-cost strategies are the most cost-effective option compared to other cost levels.

To our knowledge, there are few studies on the optimal control problem in size-structured epidemic models. Comparing these models with those for age-structured models, we observed that the only difference lies in the persistence of the non-constant function $g(\cdot)$. The age-structured model is a special case of the size-structured model when $g(\cdot) = 1$. The study of an age-structured influenza model demonstrated that low-cost vaccination can balance the outcomes of the prevention strategies [42]. Unlike our findings, while antiviral treatment lowers the viral load in individuals, it causes the number of influenza cases to rise. The size-structured model encounters difficulties in dy-

namic analysis of the coupled models because the growth of structural variables does not follow a monotonic trend over time. The inclusion of $g(\cdot)$ significantly alters the numerical results of the epidemic model, suggesting that when an individual's size grows asynchronously with time, it introduces new challenges to both the dynamical behavior and numerical simulation results of the system.

However, due to the lack of clinical data on influenza cases classified by viral load, and the optimal strategy's differential step size proposed in this paper is definite, which limits its applicability to more complex practical scenarios. Additionally, we have not yet examined the impact of simultaneous influenza and pneumonia infection on the optimal control. These aspects will be left for further research.

Acknowledgments

This work was partially supported by the Humanities and Social Foundation of Ministry of Education of China (Grant No. 22YJAZH129), by the National Natural Science Foundation of China (Grant Nos. 12271143, 12571536), by the Shanxi Scholarship Council of China (Grant No. 2023-024).

References

[1] F. B. Agusto, *Optimal isolation control strategies and cost-effectiveness analysis of a two-strain avian influenza model*, Biosystems, 113(3):155–164, 2013.

[2] P. Baccam et al., *Kinetics of influenza a virus infection in humans*, J. Virol., 80(15):7590–7599, 2006.

[3] S. Bhattacharya, M. Martcheva, and X.-Z. Li, *A predator-prey-disease model with immune response in infected prey*, J. Math. Anal. Appl., 411(1):297–313, 2014.

[4] A. Boianelli et al., *Modeling influenza virus infection: A roadmap for influenza research*, Viruses, 7(10):5274–5304, 2015.

[5] A. C. Boon et al., *H5N1 influenza virus pathogenesis in genetically diverse mice is mediated at the level of viral load*, mBio, 2(5):e00171–11, 2011.

[6] X. Cen, Z. Feng, and Y. Zhao, *Emerging disease dynamics in a model coupling within-host and between-host systems*, J. Theor. Biol., 361:141–151, 2014.

[7] T. K. Cheung and L. L. Poon, *Biology of influenza a virus*, Ann. N. Y. Acad. Sci., 1102(1):1–25, 2007.

[8] L. M. Childs et al., *Linked within-host and between-host models and data for infectious diseases: A systematic review*, PeerJ, 7:e7057, 2019.

[9] M. Clements, R. Betts, E. Tierney, and B. Murphy, *Serum and nasal wash antibodies associated with resistance to experimental challenge with influenza a wild-type virus*, J. Clin. Microbiol., 24(1):157–160, 1986.

[10] O. Diekmann, J. A. P. Heesterbeek, and J. A. J. Metz, *On the definition and the computation of the basic reproduction ratio R_0 in models for infectious diseases in heterogeneous populations*, J. Math. Biol., 28:365–382, 1990.

[11] N. Dorratoltaj et al., *Multi-scale immunoepidemiological modeling of within-host and between-host HIV dynamics: Systematic review of mathematical models*, PeerJ, 5:e3877, 2017.

[12] R. Farrukee and A. C. Hurt, *Antiviral drugs for the treatment and prevention of influenza*, Curr. Treat. Options Infect. Dis., 9:318–332, 2017.
[13] M. A. Gilchrist and A. Sasaki, *Modeling host-parasite coevolution: A nested approach based on mechanistic models*, J. Math. Biol., 218(3):289–308, 2002.
[14] A. Granados et al., *Influenza and rhinovirus viral load and disease severity in upper respiratory tract infections*, J. Clin. Virol., 86:14–19, 2017.
[15] L. A. Grohskopf et al., *Prevention and control of seasonal influenza with vaccines: Recommendations of the Advisory Committee on Immunization Practices, United States, 2020–21 influenza season*, MMWR Recomm. Rep., 69(8):1–24, 2020.
[16] H. Gulbudak and C. J. Browne, *Infection severity across scales in multi-strain immuno-epidemiological dengue model structured by host antibody level*, J. Math. Biol., 80(6):1803–1843, 2020.
[17] A. Handel et al., *A multi-scale analysis of influenza a virus fitness trade-offs due to temperature-dependent virus persistence*, PLoS Comput. Biol., 9(3):e1002989, 2013.
[18] H. R. Joshi, *Optimal control of an HIV immunology model*, Optim. Control Appl. Methods, 23(4):199–213, 2002.
[19] C. W. Kanyiri, L. Luboobi, and M. Kimathi, *Application of optimal control to influenza pneumonia coinfection with antiviral resistance*, Comput. Math. Methods Med., 2020(1):5984095, 2020.
[20] E. D. Kilbourne, *Influenza pandemics of the 20th century*, Emerg. Infect. Dis., 12(1):9, 2006.
[21] T. Kostova, *Persistence of viral infections on the population level explained by an immunoepidemiological model*, Math. Biosci., 206(2):309–319, 2007.
[22] S. Lee, G. Chowell, and C. Castillo-Chávez, *Optimal control for pandemic influenza: The role of limited antiviral treatment and isolation*, J. Theor. Biol., 265(2):136–150, 2010.
[23] X.-Z. Li, J. Yang, and M. Martcheva, *Age Structured Epidemic Modeling*, in: Interdisciplinary Applied Mathematics, Vol. 52, Springer, 2020.
[24] W. G. Lindsley et al., *Viable influenza a virus in airborne particles from human coughs*, J. Occup. Environ. Hyg., 12(2):107–113, 2015.
[25] M. Martcheva, *An Introduction to Mathematical Epidemiology*, in: Texts in Applied Mathematics, Vol. 61, Springer, 2015.
[26] M. Martcheva, N. Tuncer, and C. St Mary, *Coupling within-host and between-host infectious diseases models*, Biomath, 4(2):1510091, 2015.
[27] R. A. Medina and A. García-Sastre, *Influenza a viruses: New research developments*, Nat. Rev. Microbiol., 9(8):590–603, 2011.
[28] L. N. Murillo, M. S. Murillo, and A. S. Perelson, *Towards multiscale modeling of influenza infection*, J. Theor. Biol., 332:267–290, 2013.
[29] B. Musundi, J. Müller, and Z. Feng, *A multi-scale model for cholera outbreaks*, Mathematics, 10(17):3114, 2022.
[30] M. A. Myers et al., *Dynamically linking influenza virus infection kinetics, lung injury, inflammation, and disease severity*, Elife, 10:e68864, 2021.
[31] S. Nanda, H. Moore, and S. Lenhart, *Optimal control of treatment in a mathematical model of chronic myelogenous leukemia*, Math. Biosci., 210(1):143–156, 2007.
[32] K. M. Neuzil et al., *Efficacy of inactivated and cold-adapted vaccines against influenza a infection, 1985 to 1990: The pediatric experience*, Pediatr. Infect. Dis. J., 20(8):733–740, 2001.
[33] E. Numfor, N. Tuncer, and M. Martcheva, *Optimal control of a multi-scale HIV-opioid model*, J. Biol. Dyn., 18(1):2317245, 2024.
[34] T. H. Oguin et al., *Phospholipase d facilitates efficient entry of influenza virus, allowing escape from innate immune inhibition*, J. Biol. Chem., 289(37):25405–25417, 2014.

[35] C. W. Potter, *A history of influenza*, J. Appl. Microbiol., 91(4):572–579, 2001.
[36] Z. Qiu and Z. Feng, *Transmission dynamics of an influenza model with vaccination and antiviral treatment*, Bull. Math. Biol., 72:1–33, 2010.
[37] S.-i. Tamura and T. Kurata, *Defense mechanisms against influenza virus infection in the respiratory tract mucosa*, Jpn. J. Infect. Dis., 57(6):236–247, 2004.
[38] J. K. Taubenberger and D. M. Morens, *1918 influenza: The mother of all pandemics*, Revista Biomédica, 17(1):69–79, 2006.
[39] J. Tchuenche, S. Khamis, F. Agusto, and S. Mpeshe, *Optimal control and sensitivity analysis of an influenza model with treatment and vaccination*, Acta Biotheor., 59(1):1–28, 2011.
[40] S. A. Valkenburg et al., *Immunity to seasonal and pandemic influenza A viruses*, Microbes Infect., 13(5):489–501, 2011.
[41] J. Yang, G. Wang, M. Zhou, and X. Wang, *Interplays of a waterborne disease model linking within-and between-host dynamics with waning vaccine-induced immunity*, Int. J. Biomath., 15(03):2250003, 2022.
[42] J. Yang, L. Yang, and L. Xue, *Optimal control of a multi-scale immuno-influenza a transmission model with viral load-dependent infection*, Appl. Math. Model., 132:1–21, 2024.
[43] K. Zhou et al., *Swift and strong NK cell responses protect 129 mice against high-dose influenza virus infection*, J. Immunol., 196(4):1842–1854, 2016.